Structural Eng./Earthquake Eng., JSCE, Vol.16, No.2, 133s-142s, 1999 October

ERROR ESTIMATION OF ABSORBING BOUNDARY CONDITION FOR TWO-PHASE GROUND

Takashi AKIYOSHI[1], Xun SUN[2] and Kunihiko FUCHIDA[3]

[1]Member of JSCE, Dr. Eng, Professor, Dept. of Civil Eng. and Arch., Kumamoto University
(2-39-1 Kurokami, Kumamoto 860-8555, Japan)
[2]M. Eng., Grad. Stu., Graduate School of Science and Technology, Kumamoto University
(2-39-1 Kurokami, Kumamoto 860-8555, Japan)
[3]Member of JSCE, Dr. Eng., Assoc. Prof., Dept. of Civil and Arch. Eng., Yatsushiro Coll. of Tech.
(2627 Hirayama-Shinmachi, Yatsushiro 866-8501, Japan)

Prior to the dynamic analysis of fluid-saturated porous media, the absorbing boundary conditions in the time domain for *u-w* formulation based on Biot's two-phase mixture theory and the paraxial approximation are presented briefly. Then applying the absorbing boundary conditions to the liquefaction analysis of a 2D dipping layer ground model, the efficiency of the proposed method is evaluated by comparing the RMS response results with the reference solution which is almost equivalent to a free field response. Numerical results for several parameters regarding the topography of the ground model and input seismic waves show the accuracy and efficiency of the proposed absorbing boundary conditions even for the nonlinear dynamic analysis of infinite fluid-saturated porous media.

Key Words *: absorbing(viscous) boundary conditions, Biot's 2-phase mixture theory, fluid-saturated porous media, paraxial approximation, liquefaction, far-field*

1. INTRODUCTION

The analysis of dynamic phenomena in fluid-saturated porous media is of great interest in geotechnical and earthquake engineering. Biot[1)] first established the framework in the formulation of the dynamic response of fluid-saturated elastic-porous media. Since then, this formulation has been frequently used for the dynamic analysis of fluid-saturated porous media. The dynamic analysis is usually implemented via numerical methods involving discretization of both spatial and temporal domains. A variety of finite element models has been developed for such problem. The typical finite element models for the dynamic analysis of solid-fluid coupled problems include the works of Ghaboussi and Wilson[2)], Zienkiewicz and Shiomi[3)], Prevost[4)], and Simon *et al.*[5)] These approaches can account for the complex geometry, inhomogeneity and nonlinear behavior. However, compared with the finite element scheme applied to the single-phase media, the computation effort increases substantially due to the additional degrees of freedom associated with the pore fluid. In order to reduce the cost of analysis, the computational model is restricted to a finite domain. Consequently, it is necessary to devise special boundary techniques to incorporate the radiation condition of the truncated unbounded domain into the finite computational model.

In the dynamic analysis of single-phase media, several techniques have been proposed. The efficient techniques are given for linear problems by the consistent boundary of Lysmer and Waas[6)]. However, these methods are frequency-dependent and thus inapplicable to the true nonlinear analysis in the time domain. In the transitory case Lysmer and Kuhlemyer[7)], White *et al.*[8)] and Akiyoshi[9)] proposed some viscous boundaries. Smith[10)] proposed the superposition boundary to eliminate boundary reflections. Clayton *et al.*[11)] proposed the paraxial boundary which can deal with more inclined waves on the boundary by simply refining the approximation.

In the dynamic analysis of fluid-saturated porous media, Modaressi and Benzenati[12),13)] proposed an

This paper is translated into English from the Japanese paper, whish originally appeared on J. Struct. Mech. Earthquake Eng., JSCE, No.619/I-47, pp.111-120, 1999.4.

absorbing boundary element for the *u-p* formulation and presented an illustrative example of the efficiency of the proposed boundary. Degrande and Roeck[14] gave an absorbing boundary condition in the frequency domain. However, the work on how to model reasonably an unbounded domain in the non-linear seismic analysis of a saturated soil-structure system seems far from adequate.

In this paper, the absorbing boundary conditions due to the *u-w* formulation in the time domain for the dynamic analysis of fluid-saturated porous media are briefly presented and devised for computation[15]. In the presentation of the absorbing boundary conditions that follows, we start with a simple derivation of a local transient impedance which is equivalent to a viscous damping dashpot, using a general solution of Biot's formulation in the time domain due to the paraxial approximation. Next, to be adaptive to the existing computation programs, the absorbing boundary conditions which are usually derived in the local coordinate system are formulated in the global Cartesian coordinate system.

So far the proposed absorbing boundary conditions have been incorporated into the 2D-FEM linear and nonlinear computation programs and have shown the effectiveness, by the direct comparison of the time histories of the finite ground models for various boundary conditions and different ways of excitations[16]. In this paper, the effectiveness of the proposed method is shown quantitatively comparing the root-mean-square errors of the responses of the inhomogeneous ground model for the absorbing boundary conditions with those for the free boundary condition.

2. GOVERNING EQUATION AND ABSORBING BOUNDARY CONDITIONS

(1)Governing equations

The equation of motion for small strain of fluid-saturated porous media was given by Biot[1]. The porous medium can be viewed as a mixture composed of solid and pore fluid phases. The dynamic equilibrium equation for the solid-fluid phase and the generalized Darcy law for the dynamic equilibrium of the pore fluid can be written as[3]

$$\left.\begin{aligned} \boldsymbol{L}^T\boldsymbol{\sigma}+\rho\boldsymbol{b}&=\rho\ddot{\boldsymbol{u}}+\rho_f\ddot{\boldsymbol{w}}\\ -\nabla p+\rho_f\boldsymbol{b}&=\rho_f\ddot{\boldsymbol{u}}+\frac{\rho_f}{n}\ddot{\boldsymbol{w}}+\frac{1}{k}\dot{\boldsymbol{w}}\end{aligned}\right\} \tag{1}$$

where a superposed dot indicates a time derivative and a vector matrix notation is used to represent

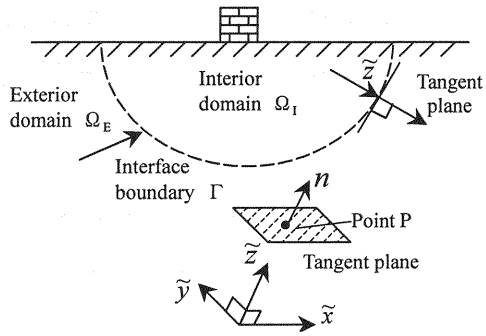

Fig.1 Typical infinite media

tensors; i.e.

$$\begin{aligned}\boldsymbol{\sigma}^T&=\left(\sigma_{xx},\sigma_{yy},\sigma_{zz},\sigma_{xy},\sigma_{yz},\sigma_{zx}\right)\\ \boldsymbol{u}^T&=\left(u_x,u_y,u_z\right),\quad \boldsymbol{w}^T=\left(w_x,w_y,w_z\right)\\ \boldsymbol{b}^T&=\left(b_x,b_y,b_z\right)\\ \nabla^T&=\left(\partial/\partial x,\partial/\partial y,\partial/\partial z\right)\\ \boldsymbol{L}^T&=\begin{bmatrix}\partial/\partial x & 0 & 0 & \partial/\partial y & 0 & \partial/\partial z\\ 0 & \partial/\partial y & 0 & \partial/\partial x & \partial/\partial z & 0\\ 0 & 0 & \partial/\partial z & 0 & \partial/\partial y & \partial/\partial x\end{bmatrix}\end{aligned} \tag{2}$$

Here, $\boldsymbol{u}$ and $\boldsymbol{w}$ are the solid phase displacement and the relative pore fluid displacement, respectively; $\boldsymbol{\sigma}$ is the total stress; $\boldsymbol{b}$ is the body force; p is the pore fluid pressure; n is the porosity; ρ and ρ_f are the density of the bulk solid-fluid mixture and the density of the pore fluid, respectively, so that $\rho=(1-n)\rho_s+n\rho_f$, where ρ_s is the density of the solid grain; k is the isotropic permeability coefficient.

The stress-strain relationship of a linear, isotropic elastic material can be written as

$$\boldsymbol{\sigma}=\boldsymbol{D}\boldsymbol{\varepsilon}-\alpha\boldsymbol{m}p \tag{3}$$

$$p=-\alpha Q\boldsymbol{m}^T\boldsymbol{\varepsilon}-Q\zeta \tag{4}$$

where $\boldsymbol{\varepsilon}=\boldsymbol{L}\boldsymbol{u}$ and $\zeta=\nabla^T\boldsymbol{w}$ are the strain in the solid and the volumetric strain in the pore fluid, respectively; $\boldsymbol{D}$ is the drained material stiffness matrix; $\boldsymbol{m}^T=(1,1,1,0,0,0)$ is equivalent to the Kronecker's delta; α and Q are related with materials through

$$\alpha=1-K_d/K_s,\quad 1/Q=n/K_f+(\alpha-n)/K_s \tag{5}$$

where K_s and K_f are the bulk moduli of the solid and pore fluid, respectively; K_d is the bulk modulus of the solid skeleton.

(2)Absorbing boundary conditions

The objective of this section is to briefly state the derivation of the absorbing boundary conditions for the dynamic analysis of fluid-saturated porous media and show the formulation for the existing 2D-FE computation programs for liquefaction[15),16)]. We now consider the infinite domain as shown in **Fig.1**. The domain is divided into two sub-domains Ω_I and Ω_E with the imaginary convex interface boundary Γ. The interior domain Ω_I is bounded. Firstly, we assume that (1) the stress, the displacement and the pore fluid flow are continuous on the interface boundary; (2) the media are linear, isotropic and homogeneous at the vicinity of the interface boundary. Next, a local dynamic impedance with respect to time and space is introduced on the interface boundary. The virtual impedance on the interface boundary represents the virtual action exerted by the exterior domain Ω_E on the interior domain Ω_I, when Ω_E is subjected to radiant waves coming from and going to the infinity. According to the definition, the impedance can be obtained by the stress and pore fluid pressure or pore fluid flow on the interface boundary.

In the dynamic analysis of single-phase media, Clayton *et al.*[11)] developed a local boundary condition which permits diffracting waves to be evacuated from the domain by use of the paraxial approximation. It was demonstrated that this approximation is very accurate for high-frequency waves and for waves impinging the boundary with a small incident angle. Now this concept is generalized into the case of fluid-saturated porous media.

We now consider an arbitrary point P on the interface boundary surface as shown in **Fig.1**. The unit outward direction $\boldsymbol{n}$ is normal to the tangent plane at the point P on the boundary surface. To simplify the derivation, we assume, without loss of the generality, that the positive z-direction of the coordinate system is the same as the outward normal direction $\boldsymbol{n}$. Therefore, the normal and tangent components of the stress vector in the tangent plane at the point P can be represented by σ_z, τ_{zx} and τ_{zy}. On the interface boundary Γ, an absorbing boundary condition in the time domain is used which approximately models the radiation of waves in an unbounded space domain. A 2-D absorbing boundary condition for the u-w formulation has been established in a local $(\tilde{x}, \tilde{z})$ Cartesian co-ordinate system where $\tilde{z}$ and $\tilde{x}$ are normal (in the direction of the outward normal $\boldsymbol{n}$) and tangential to the boundary, respectively. The absorbing boundary condition establishes a relation between stresses and displacements, and can be considered as a mixed boundary condition, i.e.

$$\{\tilde{\tau}_{zx}, \tilde{\tau}_{zy}, \tilde{\sigma}_z, 0, 0, -\tilde{p}\} = -\begin{bmatrix} \mathbf{c}_{uu} & \mathbf{c}_{uw} \\ \mathbf{c}_{uw}^T & \mathbf{c}_{ww} \end{bmatrix} \begin{Bmatrix} \dot{\tilde{\mathbf{u}}} \\ \dot{\tilde{\mathbf{w}}} \end{Bmatrix} \tag{6}$$

with

$$c_{uu} = \begin{bmatrix} \rho V_3 & 0 & 0 \\ 0 & \rho V_3 & 0 \\ 0 & 0 & \rho V_1 \end{bmatrix}, \quad c_{uw} = \begin{bmatrix} 0 & 0 & 0 \\ 0 & 0 & 0 \\ 0 & 0 & \alpha Q/V_1 \end{bmatrix}$$
$$c_{ww} = \begin{bmatrix} 0 & 0 & 0 \\ 0 & 0 & 0 \\ 0 & 0 & Q/V_1 \end{bmatrix} \tag{7}$$

and $V_1 = \sqrt{(\lambda + 2G + \alpha^2 Q)/\rho}$, $V_3 = \sqrt{G/\rho}$ where λ and G are the Lame's constants and G is also called the shear modulus. However, for the nonlinear computation such as liquefaction, G will change with time because the effective stress of materials depends on the pore fluid pressure.

From the above absorbing boundary conditions, it can be seen that the zeroth-order paraxial boundaries correspond to consistent dampers. Therefore, it can be noted that these absorbing boundaries are also equivalent to the viscous boundaries.

As the absorbing boundary condition is defined in a local $(\tilde{x}, \tilde{z})$ Cartesian co-ordinate system, a co-ordinate transformation from the local $(\tilde{x}, \tilde{z})$ to the global (x, z) Cartesian co-ordinate system is needed. Hence, a projection matrix $\boldsymbol{P}$ which relates a vector $\boldsymbol{v}$ given in the local Cartesian co-ordinate system on the absorbing boundary to the global Cartesian co-ordinate system $\boldsymbol{v}$ is defined as

$$\tilde{\boldsymbol{v}} = \boldsymbol{P}\boldsymbol{v} \tag{8}$$

By using the projection matrix $\boldsymbol{P}$ for equation (6) and considering the motion of the free field during earthquake, the absorbing boundary condition in the global Cartesian co-ordinate system can be given by

$$\begin{Bmatrix} \bar{\boldsymbol{t}} \\ -\bar{p}\boldsymbol{n} \end{Bmatrix} = \begin{Bmatrix} \bar{\boldsymbol{t}}^f \\ -\bar{p}^f \boldsymbol{n} \end{Bmatrix} - \begin{bmatrix} \boldsymbol{P}^T \boldsymbol{c}_{uu} \boldsymbol{P} & \boldsymbol{P}^T \boldsymbol{c}_{uw} \boldsymbol{P} \\ \boldsymbol{P}^T \boldsymbol{c}_{uw}^T \boldsymbol{P} & \boldsymbol{P}^T \boldsymbol{c}_{ww} \boldsymbol{P} \end{bmatrix} \begin{Bmatrix} \dot{\boldsymbol{u}} - \dot{\boldsymbol{u}}^f \\ \dot{\boldsymbol{w}} - \dot{\boldsymbol{w}}^f \end{Bmatrix} \tag{9}$$

where a superscript f on a variable means the contribution from the motion of the free field; $\bar{\mathbf{t}}$ and $\bar{p}$ represent the traction and the pore water pressure on the boundary Γ, respectively.

Incorporation of eqn.(9) for liquefaction analysis requires simultaneous computations for a finite field model and a free field model. For a single-phase ground mode, the proposed absorbing boundary due to u-w formulation will reduce to the Miura and Okinaka's method[17)].

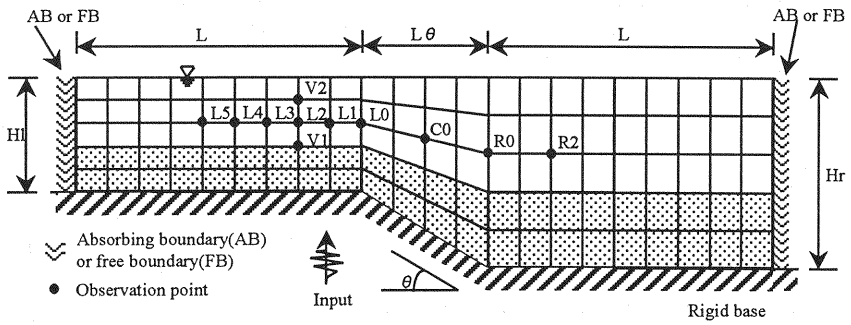

Fig.2 2D saturated dipping layer FE model subjected to vertical s eismic wave

3. APPLICATION OF ABSORBING BOUNDARY CONDITION TO GROUND MODELS

(1) Ground models for computation and reference solutions

In order to verify the accuracy and efficiency of the proposed absorbing boundary condition, the analysis of the saturated soil deposits are performed. The proposed method is incorporated into the finite element computer program NUW2[16] for which the correctiveness and the efficiency have been proved using a simple ground model and the closed form solution in time domain. In the calculations, following assumptions are used; (1)the four-node bilinear isoparametric element is used under the plain strain condition. (2)The Newmark parameters in the integration scheme are chosen as γ=0.60 and β=0.3025 in order not to obscure the interpretation of the results. This choice for γ introduces a slight numerical damping and the selected value for β maximizes high frequency numerical dissipation. No additional viscous physical damping is introduced, except the absorbing boundary. (3)The ground surface is drainable.

The standard ground model for computation shown in **Fig.2** does not have a closed form solution. Hence in the estimation of the correctiveness of the absorbing boundary condition, the reference solution model is defined to be so wide that the reflected waves from side boundaries can not reach the observation sites during earthquakes. The ground model is the 2D dipping surface layer model of two saturated porous media with different initial shear moduli, resting on the rigid base rock and subject to vertical random waves simultaneously. The soil parameters of these two layers are interpolated from the triaxial test results, shown in **Table 1**, in which

Table 1 Soil parameters for liquefaction analysis

Parameters	Upper layer	Lower layer
G_{m0}(kPa)	22990	65030
p_1	0.50	0.50
p_2	0.80	1.40
w_1	2.80	7.20
S_1	0.005	0.005
c_1	1.60	1.70
ϕ_f'(degree)	31	37
ϕ_p'(degree)	28	28
H_m	0.30	0.30

the parameters follow the Iai's constitutive model[18),19)]. In the geography of the model, the elements are of 5m x 5m in the right wing layer and 5m x 5m in the left wing layer, and the length of both wings are L=50m, and the horizontal length of the dipping layer is Lθ=20m, and therefore the total horizontal length is 120m. The thicknesses of the surface layers are 25m in the right wing layer and 15m in the left wing layer.

As the inputs vertically impinging to the bottom boundary of the surface layer, El Centro earthquake (1940, NS component, maximum acceleration amplitude=0.2g) is used mainly whereas Hyogo-ken Nanbu Earthquake (1995), Chiba-ken Toho-oki Earthquake (1987) and Tokachi-oki earthquake (1968) are used auxiliary.

For the reference solution, the ground model with the wing length of 1,000m is adopted because the average shear wave velocity is about 160m/s and thus reflected waves does not reach the observation site within 10 seconds which is enough time for the main vibration. In Fig.2 and hereafter, the boundary condition is represented as FB for free boundary condition and as AB for absorbing boundary condition.

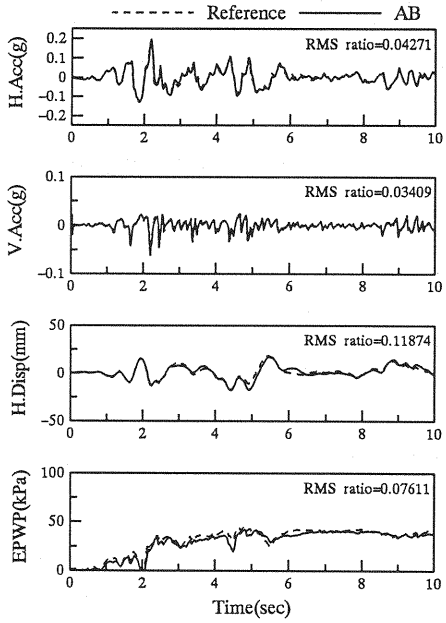

Fig.3 Responses with absorbing boundary at point L0

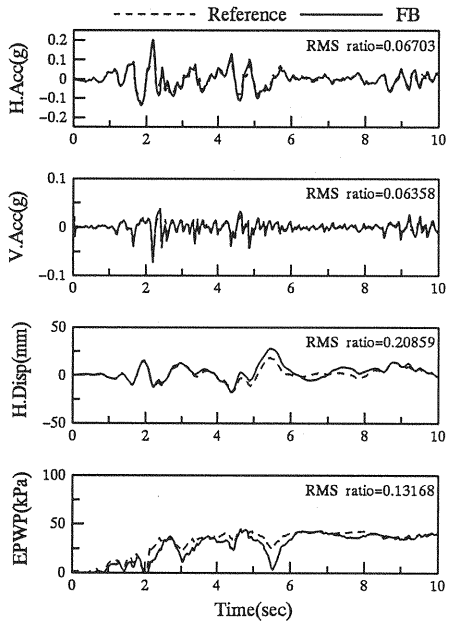

Fig.4 Responses with free boundary at point L0

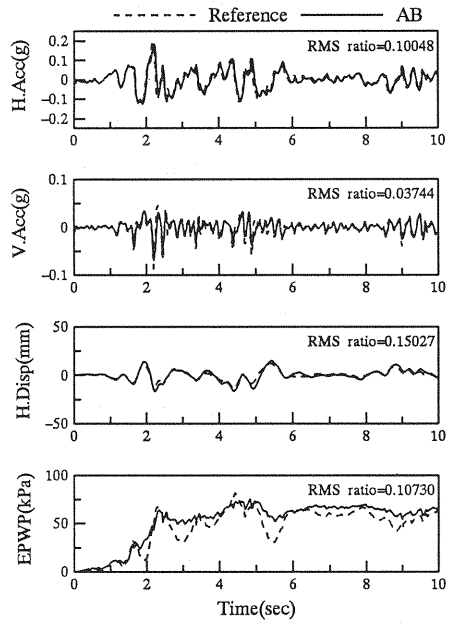

Fig.5 Responses with absorbing boundary at point R0

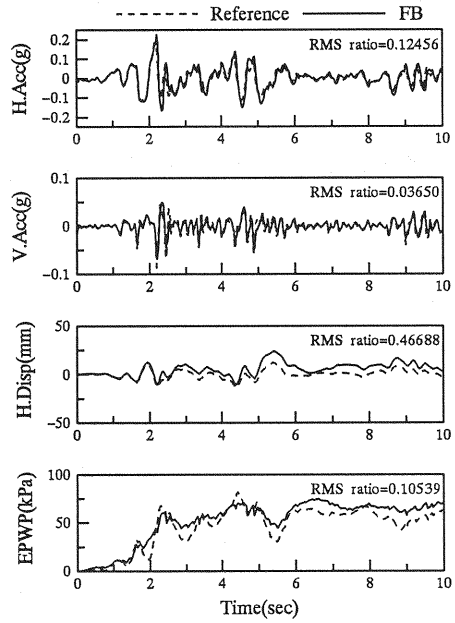

Fig.6 Responses with free boundary at point R0

(2) Application to 2D dipping layer ground models

The 2D dipping ground model for computation (**Fig.2**) is equipped AB or FB at the vertical side bondaries, and L0 is the observation or reference point. In the diagrams shown later H.Acc, V.Acc, H.Disp and EPWP represent the horizontal acceleration, the vertical acceleration, the horizontal displacement and the excess pore water pressure, respectively.

Fig.3 shows the results of the response of the ground model at point L0 for El Centro Earthquake,

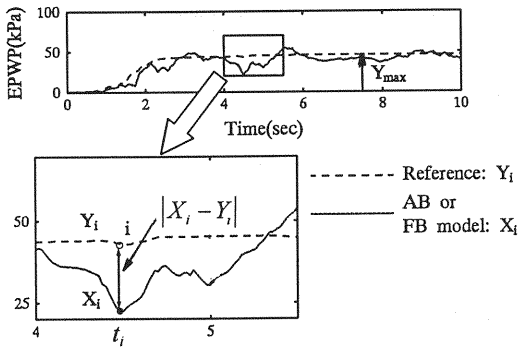

Fig.7 Differences between absorbing boundary and reference solution

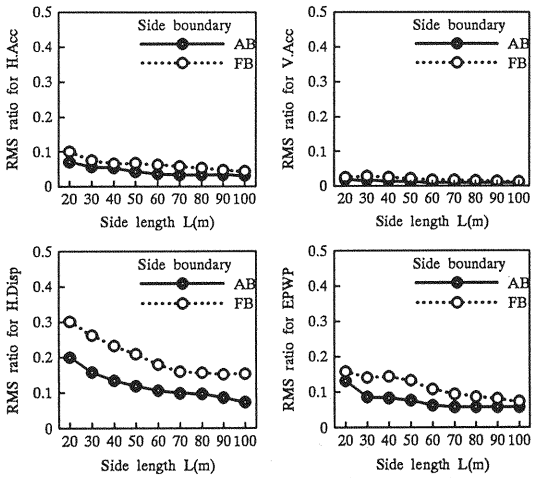

Fig.8 RMS ratio versus side length of parallel layers

in which the time history of AB model (:solid lines) is compared with the reference solution (:dotted lines). Little difference between both time histories can be seen in this case. However, a considerable difference between the time histories of FB model (:solid lines) and the reference solution (:dotted lines) can be seen in **Fig.4**, especially for the responses of the vertical acceleration (:V.Acc), the horizontal displacement (:H.Disp) and the pore water pressure (:EPWP). Both diagrams show that the proposed absorbing boundary condition gives more accurate solutions than the free boundary condition, even for the liquefaction as one of nonlinear problems.

Figs.5 and **6** show the same amplitudes as in **Figs.3** and **4**, but for the observation point R0, and the efficiency of AB model is obtained.

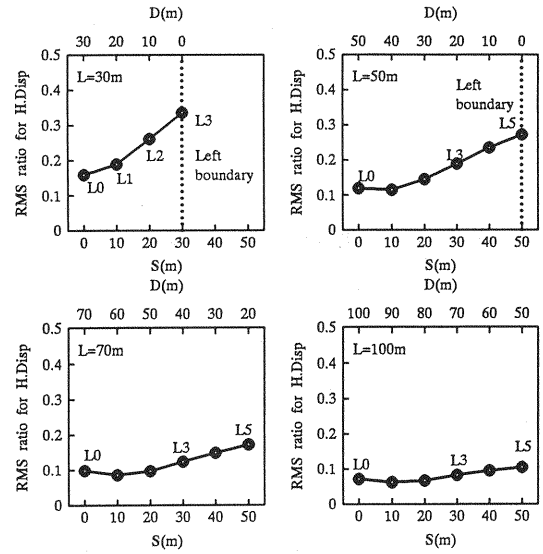

Fig.9 RMS ratio for horizontal displacement versus relative distance S or D (with absorbing boundary)

4. ERROR ESTIMATION OF ABSORBING BOUNDARY CONDITION FOR NONLINEAR 2-PHASE PROBLEMS

(1)Quantitative error estimation

For the quantitative estimation of the relative error of the seismic responses of the AB model or FB model to the reference solution, the RMS (:root mean square) value is defined as shown in **Fig.7**;

$$\mathrm{RMS}=\sqrt{\left(\sum_{i=1}^{N}(X_i-Y_i)^2\right)/N} \qquad (10)$$

where X_i is the time history of AB model or FB model at time t_i, Y_i is the time history of reference solution at time t_i, N is the number of digitized time.

For the nondimensional comparison of the relative errors between the responses of ground models and the reference solutions, RMS ratio which is defined as the ratio of RMS of relative errors to RMS of reference solutions is used hereafter.

(2) Influence of the length of the wing layer

In this section the influence of the length of the wing layer in the ground model (:**Fig.2**) on the results of analysis is investigated. **Fig.8** shows RMS ratios for the cases of AB model and FB model at the observation point L0 in the finite ground model, for the variation of the wing layer's length of L=20 to 100m. Upper two diagrams which correspond RMS ratios of H.Acc and V.Acc for the cases of AB or FB,

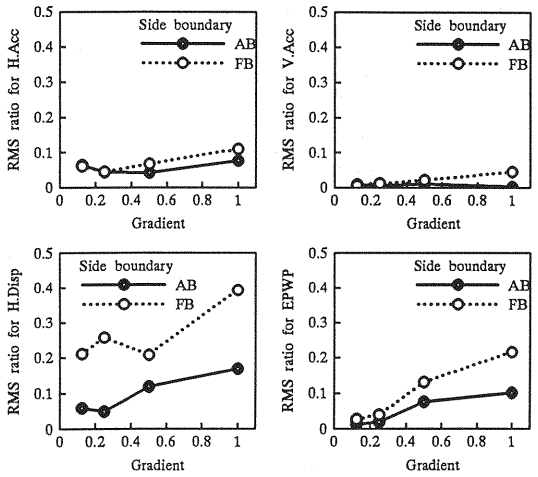

Fig.10 RMS ratio at L0 versus gradient of base surface

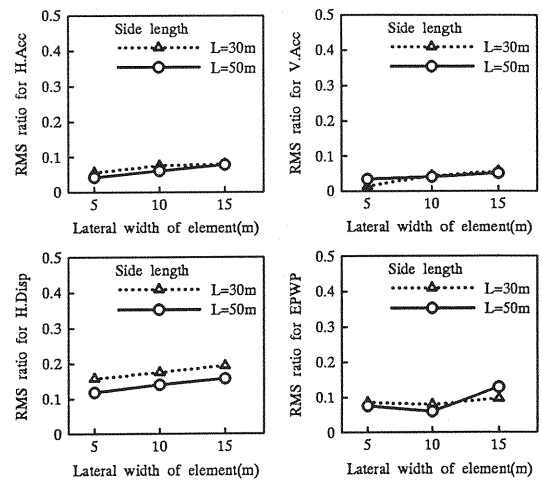

Fig.11 RMS ratio versus lateral width of element (with absorbing boundary)

and lower two diagrams which represent RMS ratios of H.Disp and EPWP for the cases of AB or FB, show that long wing length decreases errors and AB is much effective than FB for reduction of errors. The results mean that RMS ratios for the case of AB are less than 0.1 when the wing is longer than 50m. For this model, the wing length of 50m gives sufficiently accurate results and can be an index value in practical use.

Fig.9 is to show the influence of the distance between the observation point and the side vertical boundary on the distribution of RMS ratios of H.Disp with AB. An internal observation point Li(i=0,1,...,5) is measured from the point L0 as S(m) and from the left-side vertical boundary as D(m)=L-S. These diagrams indicate that RMS error increases as the observation point approaches the boundary. Therefore in order to reduce errors, some distance between the observation point and the side boundary must be kept. As long as these examples, at least the distance of 30m between the observation point and the left side boundary face is required to keep RMS ratio under 0.15.

(3) Influence of the dipping angle at the bottom interface

This section investigates the influence of the dipping angle of the interface on the seismic response of the surface layer. **Fig.10** is the plots of RMS ratios for H.Acc, V.Acc, H.Disp and EPWP at the observation point L0 versus Gradient, which is defined as the dipping angle measured from the horizontal surface of the bottom interface in the surface layer. It is reasonable to explain that a large dipping angle of the central layer induces reflected waves in multi-directions, then reduces the absorbing effect of the side boundaries due to the large incident angles to the side boundaries[15], and finally produces a marked difference between responses of the ground models and the reference models. This tendency appears especially for H.Disp and EPWP, and also for the case of the free boundary. However, for the case of the absorbing boundary, RMS ratio of the relative error falls under 0.1 which will be negligibly small in practical use, for the gradient less than 0.5.

(4) Influence of the elemental width

Increasing elemental width for a given wave length is expected to make a high-cut filter and increases the relative error. In **Fig.11**, H.Acc, V.Acc, H.Disp and EPWP at the observation point L0 are plotted, for the variable elemental lateral width under the constant elemental height (:5m). Four diagrams show that RMS ratios in the errors seem to be insensitive to the elemental width and the proposed absorbing boundary condition offers the stable results of analysis.

(5) Influence of the soil stiffness

Fig.12 is the time histories with AB at the observation point L0, in which the initial physical property of the ground model is uniform, consisting of the lower layer's soil parameters in **Table 1**. The plots of acceleration and displacement are almost similar with the results in **Fig.3** for the standard ground model using the soil parameters of **Table 1**,

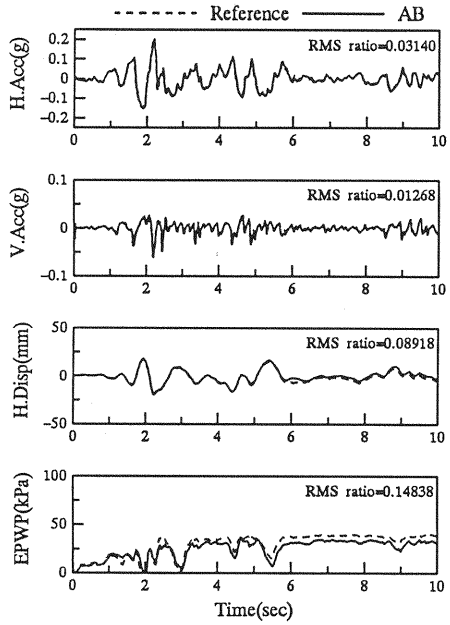

Fig.12 Responses with absorbing boundary at point L0

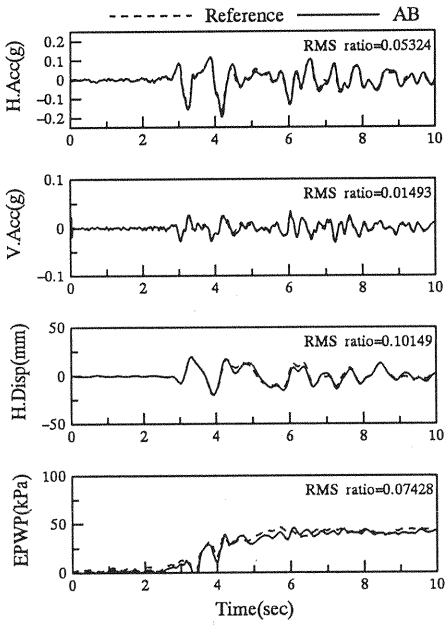

Fig.14 Responses with absorbing boundary at point L0 (Hyogo-ken Nanbu Earthquake)

except for a small error in the pore pressure. This means that the absorbing boundary works effectively for smooth transmission of waves of acceleration and displacement through the fictitious boundaries and the time histories of the surface layer are not sensitive for the difference of physical properties of

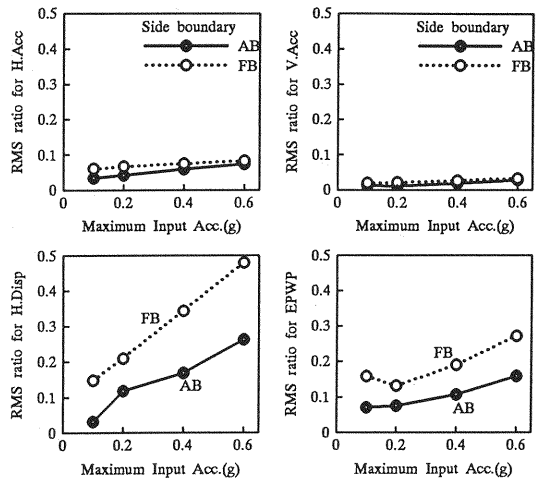

Fig.13 RMS ratio at point L0 versus maximum Input acceleration

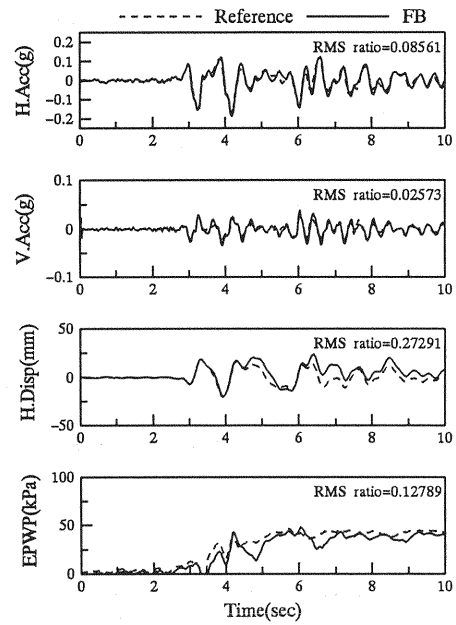

Fig.15 Responses with free boundary at point L0 (Hyogo-ken Nanbu Earthquake)

soil deposits, except for the pore water pressure.

(6) Influence of the input earthquake waves

Fig.13 is RMS ratio of the four responses of H.Acc, V.Acc, H.Disp and EPWP at the observation point L0 in the standard ground model(**Fig.2**) versus maximum acceleration amplitude of the input. RMS ratio of the response accelerations is almost independent of the variation of the maximum

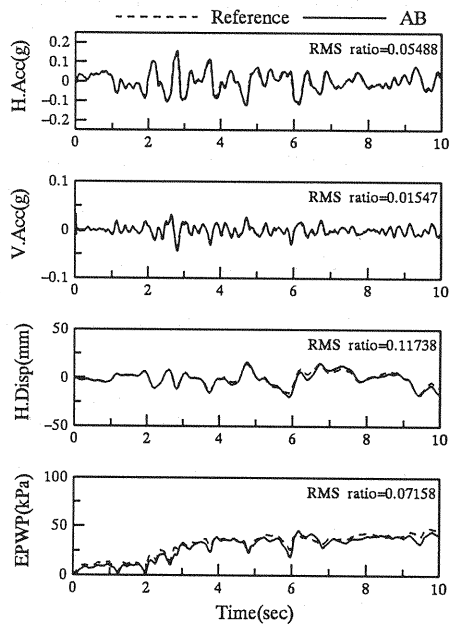

Fig.16 Responses with absorbing boundary at point L0 (Chiba-ken Toho-oki Earthquake)

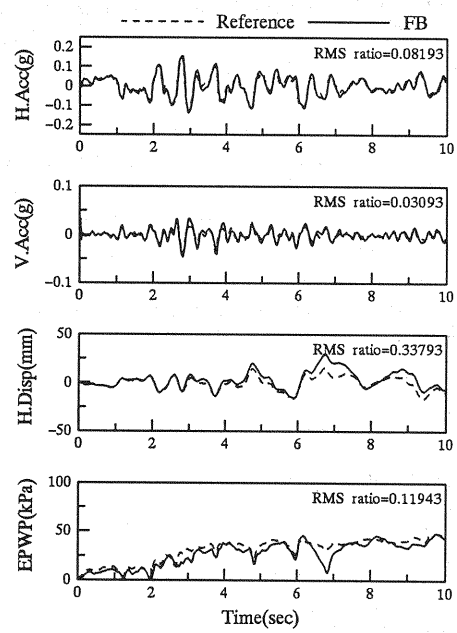

Fig.17 Responses with free boundary at point L0 (Chiba-ken Toho-oki Earthquake)

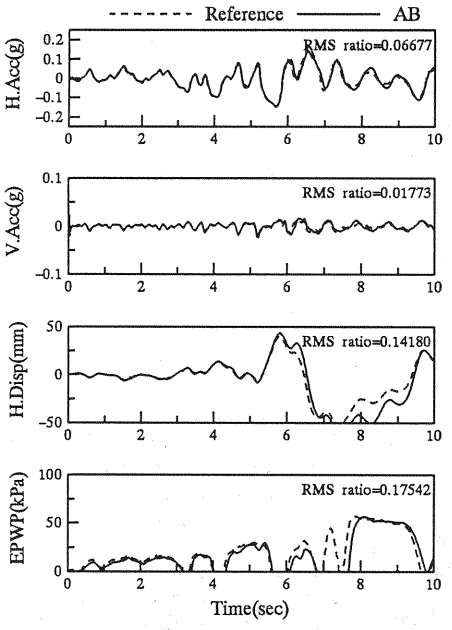

Fig.18 Responses with absorbing boundary at point L0 (Tokachi-oki Earthquake)

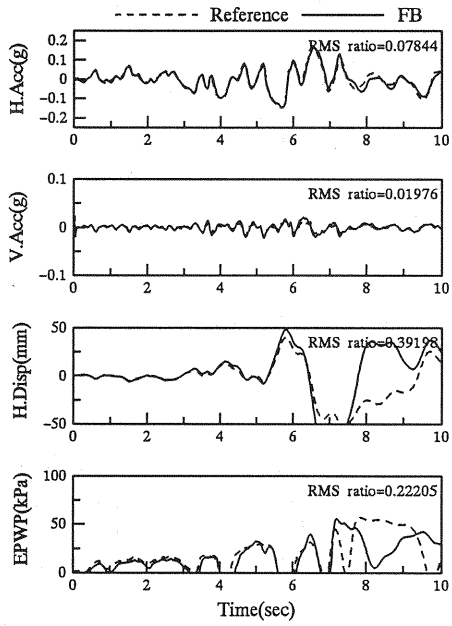

Fig.19 Responses with free boundary at point L0 (Tokachi-oki Earthquake)

amplitude of input acceleration. However, displacement and pore water pressure without AB are highly dependent on the input acceleration, compared with those with AB.

Figs.14 to **19** are the time histories at the observation point L0 in the standard ground model for three earthquakes of the maximum acceleration amplitudes of 0.2g, in which **Figs.14** and **15** are computed for a recorded time history of Hyogo-ken Nanbu Earthquake (1995), **Figs.16** and **17** for Chiba

-ken Toho-oki Earthquake (1987), and **Figs. 18** and **19** for Tokachi-oki Earthquake (1968). Those diagrams show almost similar trend with **Figs.3** and **4** which are the response of the same standard ground model subjected to El Centro Earthquake (1940). With respect to the acceleration, the proposed absorbing boundary condition produces less error for the reference solution than the free boundary condition. Regarding displacement and pore water pressure, the proposed boundary condition clearly controls the occurrence of the computational error compared with the free boundary.

5. CONCLUTIONS

An absorbing boundary condition for 2D saturated porous media is presented and shows the equivalence to a viscous damper in time domain by an approximate *u-w* formulation based on Biot's 2 phase mixture theory. To verify the efficiency of proposed absorbing boundary condition, a finite ground model with a dipping interface in the central region and with the absorbing condition or the free condition at the side vertical boundary is devoted to computation for several recorded earthquakes. Numerical computation is performed mainly for the verification of the efficiency of the proposed method for the nonlinear (liquefaction) problems, comparing the root-mean-square relative errors of the response of the finite ground model having the absorbing boundary or the free boundary to the reference solution. Results are summarized as follows;

(1) The proposed absorbing boundary condition works very efficiently and high precisely for the nonlinear analysis of saturated porous media.

(2) The absorbing boundary condition presents sufficiently accurate results by using the wing layer of 50m for the ground models in this study.

(3) Even for the topographically nonuniform case of the dipping interface, the absorbing boundary condition gives stable and accurate results as well as the reference solutions.

(4) Even for different types of earthquakes, the absorbing boundary condition shows the efficiency in practical use.

REFERENCES

1) Biot,M.A. : Theory of propagation of elastic waves in a water- saturated porous solid, part I- low frequency range; part II- higher frequency range, *J. of Acoust. Soc. Ame.*, Vol.28, pp.168-191, 1956.
2) Ghaboussi,J. & Wilson,E.L. : Variational formulation of dynamics of fluid- saturated porous elastic solids, *J. Eng. Mech. Div.*, ASCE, Vol.104, No.4, pp.947-963, 1978.
3) Zienkiewicz,O.C. & Shiomi,T. : Dynamic behavior of saturated porous media: The generalized Biot formulation and its numerical solution, *Int. J. Numer. Anal. Methods Geomech.*, Vol.8, pp.71-96., 1984.
4) Prevost,J.H. : Wave propagation in fluid- saturated porous media: An efficient finite element procedure, *Int. J. Soil dyn. and Earthq. Eng.*, Vol.4, pp.183-202, 1985.
5) Simon,B.R., Zienkiewicz,O.C. & Paul,D.K. : Evaluation of *u-w* and *u- π* finite element methods for the dynamic response of saturated porous media using one-dimensional models, *Int. J. Num. Anal. Methods Geomech.*, Vol.10, pp.461-482, 1986.
6) Lysmer,J. & Waas,G. : Shear waves in plane infinite structures, *J. Eng. Mech. Div.*, ASCE, Vol.98, No.1, pp.85-105, 1972.
7) Lysmer,J. & Kuhlemeyer,R.L. : Finite dynamic model for infinite media, *J. Eng. Mech. Div.*, ASCE, Vol.95, No.4, pp.859-877, 1969.
8) White,W., Valliappan,S. & Lee,I.K. : Unified boundary for finite dynamic models, *J. Eng. Mech. Div.*, ASCE, Vol.103, No.5, pp.949-964, 1977.
9) Akiyoshi,T. : Compatible viscous boundary for discrete models, *J. Eng. Mech. Div.*, ASCE, Vol.104, No.5, pp.1252-1265, 1978.
10) Smith,W.D. : A nonreflecting plane boundary for wave propagation problems, *J. Comp. Phys.*, Vol.15, pp.492-503, 1974.
11) Clayton,R. & Engquist,B. : Absorbing boundary conditions for acoustic and elastic wave equations, *Bull. Seism. Soc. America*, Vol.67, No.6, pp.1529-1540, 1977.
12) Modaressi,H. & Benzenati,I. : An absorbing boundary element for dynamic analysis of two- phase media, *Proc. 10WCEE*, pp. 1157-1161, 1992.
13) Modaressi,H. & Benzenati,I. : Paraxial approximation for poroelastic media, *Int. J. Soil Dyn. and Earthq. Eng.*, Vol.13, pp.117-129, 1994.
14) Degrande,G. & De Roeck,G. : An absorbing boundary condition for wave propagation in saturated poroelastic media - Part I: Formulation and efficiency evaluation; Part II: Finite element formulation, *Int. J. Soil Dyn. and Earthq. Eng.*, Vol.12, pp.411-432, 1993.
15) Akiyoshi,T., Fuchida,K. & Fang, H.L.: Absorbing boundary conditions for dynamic analysis of fluid-saturated porous media, *Int. J. Soil Dyn. and Earthq. Eng.*, Vol.13, pp.387-3 97, 1994.
16) Akiyoshi,T., Fang, H.L., Fuchida,K. & Matsumoto,H.: A non- linear seismic response analysis method for saturated soil- structure system with absorbing boundary, *Int. J. Numeri. and Analy. Meth. in Geomech.*, Vol.20, pp.307-329, 1996.
17) Miura, F. & Okinaka, H.: Dynamic analysis method for a 3-D soil-structure interaction systems with the viscous boundary based on the principle of virtual work, *Div. Earthq. Eng. and Structure, Proc. JSCE,* No.404/I-11, pp.395-404, 1989 (in Japanese).
18) Iai,S. Matsunaga,Y. & Kameoka,T. : Strain space plasticity model for cyclic model for cyclic mobility, *Soils and Foundations*, Vol.32, No.2, pp.1-15, 1992.
19) Iai,S. Matsunaga,Y. & Kameoka,T. : Analysis of undrained cyclic behavior of sand under anisotropic consolidation, *Soils and Foundations*, Vol.32, No.2, pp.16-20, 1992.